2015 International Symposium on Nonlinear Theory and its Applications
NOLTA2015, Kowloon, Hong Kong, China, December 1-4, 2015

Modelling Optical Illusions from Radially Periodic Images

Kim Minsam† and K. Y. Michael Wong‡

†Department of Computer Science and Engineering, Hong Kong University of Science and Technology
Sai Kung, Clear Water Bay, Hong Kong SAR, P. R. China
‡Department of Physics, Hong Kong University of Science and Technology
Sai Kung, Clear Water Bay, Hong Kong SAR, P. R. China
Email: mkimac@ust.hk, phkywong@ust.hk

Abstract – In 2013, study on flickering wheel illusion by R. Sokoliuk and R. VanRullen claimed that the illusion's flickering frequency corresponds to that of alpha wave which is particularly prevalent in human brain's visual cortex. This paper investigates the theoretical counterpart of the claim by modelling the orientation sensitive neural network with continuous attractor neural network (CANN) model. CANN is known for its capability of producing rich dynamics and incorporating the effects of global inhibition and short-term synaptic depression. Therefore, the illusory effect was modelled and studied by tuning the parameters of the two effects and the radial periodicity of the image stimuli. The study revealed the radial periodicity of the image can invoke various types of illusion other than flickering, and such additional effects were also generated by the simulation, and studied based on the modified actual images and virtual image inputs.

1. Introduction

1.1. Flickering Wheel Illusion

Recent study [1] on an optical illusion called 'flickering wheel illusion' reported that brain's sampling behavior of optical input causes the illusion of a static wheel-shaped image flicker at a rate significantly resembling that of occipital alpha rhythm (8 ~ 13 Hz) . (Figure 1: to

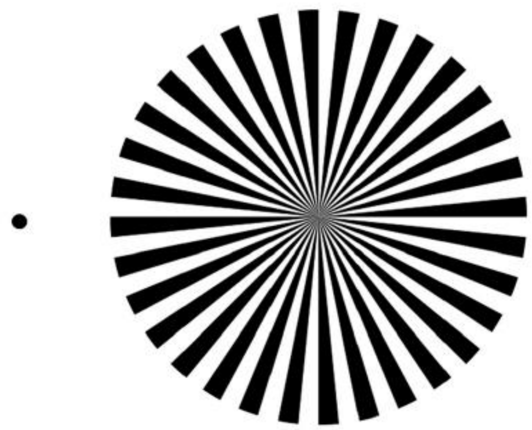

Figure 1

experience the illusion, focus on the left dot, or any other point to locate the wheel in the peripheral vision.)

Subjects in the psychophysical experiment were asked to match the flickering frequency of the stimulus with reference controlled animation. The number of spokes in the wheel, degree of contrast between spoke and empty space were varied, and subjects' brain activity was recorded by EEG at the same time. The distribution of estimated frequency was peaked at 9Hz, and flickering intensity was highest when the wheel had 32 spokes and with maximum contrast of black and white.

The occipital alpha rhythm is one of various neural oscillations in human brain. The rhythm has been widely studied using the electroencephalography, and studies of [2] and [3] show that the rhythm closely interacts with the visual information processing. More specifically, it has been shown that the visual attention consists of periodic sampling which is synchronous to the occipital alpha rhythm. Furthermore, there could be other various forms of illusion due to the radial periodicity of the image. For instance, by staring into the center of figure 2, it is

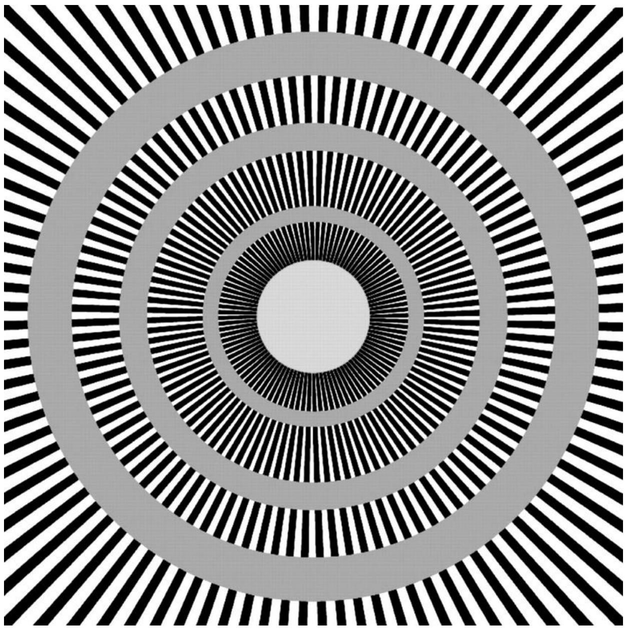

Figure 2

possible to perceive the sense of rotation within the gray slabs.

Normally, there lies a mechanism in the brain that naturally fades away the sampling periodicity from our perception. Otherwise, the entire world would be flickering in our vision. Interestingly, it turns out that the flickering optical illusion occurs when the mechanism fails to operate for certain types of visual input that shows radial periodicity like figure 1.

1.2. Neural Dynamics

Neural networks are simulated with one-dimensional continuous attractor neural network structure, adopted by [4]. The model incorporates the dynamics of 256 neurons in a ring structure so that each of the neuron responds to an orientation, or a spoke in the image, making the neuron orientation-sensitive.

First, the dynamics of the synaptic input to a particular neuron is provided by equation below.

$$\tau_s \frac{\partial u(x,t)}{\partial t} = I_{ext}(x,t) + \rho \int_{-\infty}^{\infty} dx' J(x,x') p(x',t) r(x',t) - u(x,t) \tag{1}$$

The synaptic input is controlled by three factors. The first term on the right hand side is the external input. The second is the total input from all other neurons in the network, or the ring (256-regular polygon) in this particular problem setting. The third term is neuron's own relaxation. On the left hand side, τ_s is the time constant typically of 1ms order. ρ is the linear neural density on the ring, and J(x, x') represents the interaction constant between a pair of neurons at location x and x', which is set to be proportional to the value of normal distribution computed at x-x'. (x-x' is the circular distance.)

$$J(x,x') = J_0 \exp[-\frac{(x-x')^2}{2a^2}] \tag{2}$$

p(x', t) in (1) is a variable that indicates the availability of nearby resources needed to send neural signal or a spike, with respect to the neuron at x'. The phenomenon when the lack of such resources limit neural outputs is called short-term synaptic depression (STD), when molecules like ATP (Adenosine Triphosphate) or neurotransmitter are depleted around location x' due to frequent signaling. The value of p is between 1 and 0, and its dynamics is expressed by equation (3).

$$\tau_d \frac{\partial p(x,t)}{\partial t} = 1 - p(x,t) - p(x,t)\tau_d \beta r(x,t) \tag{3}$$

τ_d is the time scale of neurotransmitter recovery, which is chosen to be $50\tau_s$. β is the variable that controls the degree of synaptic depression, and this is set to be one of independent variables in the later experiments.

Finally, r(x',t) in (1) and (3) is the firing rate of the neuron at x', which is determined by equation (4) below.

$$r(x,t) = \frac{u(x,t)^2}{1 + k\rho \int_{-\infty}^{\infty} dx' u(x',t)^2} \tag{4}$$

The equation (4) indicates that the output of a neuron is determined by the squared synaptic input divided by a term to incorporate the concept of global inhibition. Unlike short-term depression that affects small region of only a few neurons, global inhibition controls larger portion of neural network's activity in order to preserve resources for other distant networks' tasks. The degree of global inhibition is controlled by k and ρ, with the logic that denser neural network are more severely inhibited by global inhibition.

Particularly for simulation of this problem, the integration is replaced by summation over 256 neurons, and the J(x, x') is appropriately modified to fit the circular structure. (1st neuron and 256th neuron must be close.)

2. Experiment Setting

As mentioned above, the 256 neurons are assumed to be the orientation-sensitive neurons that correspond to an angle. In order to generate the effect of figure 1, the spatial input for the 256 neurons were set to be the bit string of [1 1 1 1 1 1 1 1 0 0 0 0 0 0 0 0 … 1 1 1 1 1 1 1 1 0 0 0 0 0 0 0 0] multiplied by an amplitude constant A, where each bit corresponds to one of the 256 neuron.

The input of the spokes in the wheel is periodically provided, or steadily flickered at 10Hz in the earlier experiments, and then added with jitter (temporal noise) to better simulate the noisy environment of human brain's sampling behavior of alpha-wave from 8Hz to 10Hz. Therefore, in this experiment, instead of providing non-flickering steady input to generate flickering illusion from the retina to visual cortex, it focuses on how the sampled input creates further impact. This is due to the result of [1] that the flickering illusion remains prevalent in the afterimage, where there is no additional physical input in the retina. In other words, sample information was deemed sufficient to analyze the effect, and thus used as a direct input in our experiments.

Furthermore, the amplitude constant A, global inhibition constant k, short-term synaptic depression constant β are scaled to the range that produced significantly diverse dynamics in a similar setting from the result of [5].

3. Experiment Result

3.1. Observed Dynamics

There were several distinct patterns derived from the model. Below graphs show the spatiotemporal information of firing rate of 256 neurons. X-axis represents the time-axis, and Y-axis the neuron identification index. Note that 256th neuron and 1st neuron are actually neighboring with each other in the ring structure.

Rotating bump (3 seconds)

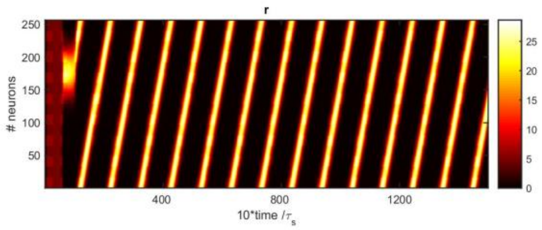

Spike (3 seconds)

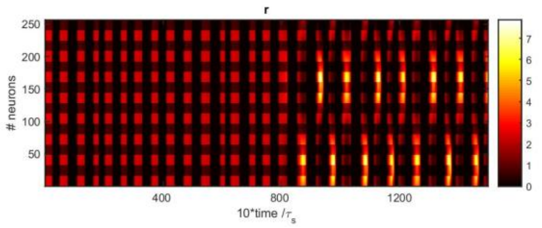

Mixed (3 seconds)

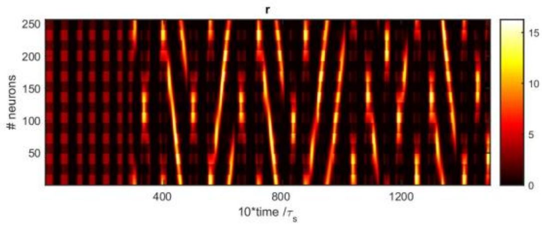

(Asynchronous) Homogeneous Spike (3 seconds)

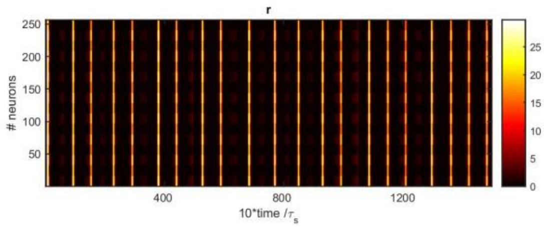

Silent (Synchronous Spike) (3 seconds)

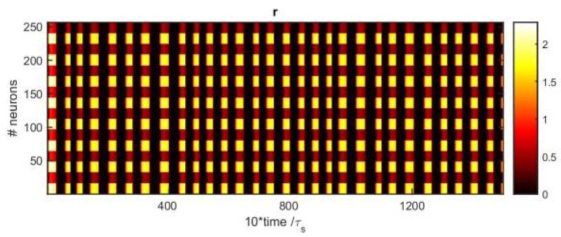

Figure 1

3.2. Impact of Parameters

Amplitude A was set to be 0.8, 1.0, and 1.2. k and beta was tested at ranges of 0.01, 0.02, … 0.05 (small scale) and 0.05, 0.15, … 0.75 (large scale). The table below summarizes the result during the first 3 seconds of simulation at amplitude 0.8, varying k and beta values in large scale. During the duration, state transitions occur, and the state in the end has been recorded.

A=0.8	k = 0.05	0.15	0.25	0.35	0.45	0.55	0.65	0.75
beta = 0.0	M	M	M	M	M	M	M	Silent
0.15	M	M	M	M	M	M	S	Silent
0.25	S	M	M	Mixed	Mixed	S	S	Silent
0.35	S	Mixed	Mixed	Mixed	S	S	Silent	Silent
0.45	S	Mixed	Mixed	S	S	Silent	Silent	Silent
0.55	HS	Mixed	S	S	Silent	Silent	Silent	Silent
0.65	HS	S	S	S	Silent	Silent	Silent	Silent
0.75	HS	S	S	Silent	Silent	Silent	Silent	Silent

Table 1. Summary of States

Repeated experiments on amplitude 1.0 and 1.2 showed minor difference. The summary certainly shows a trend, but additional information other than the summary required experiments of longer duration.

3.3. Experiments with Longer Duration

At some parameter setting, 3-second duration was not enough to view the convergence of the state, and longer-duration experiments presented better results. Results below present 10-second duration result, at amplitude A = 0.8, k = 0.15, and beta varying from 0.05 to 0.75.

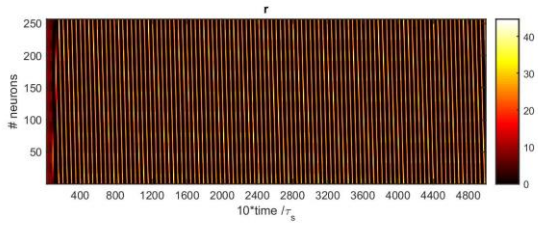

(1) Beta = 0.05: Rotating bump

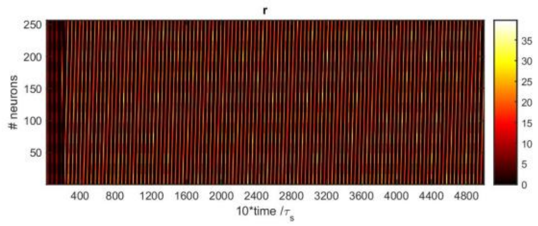

(2) Beta = 0.15: Rotating bump, faster

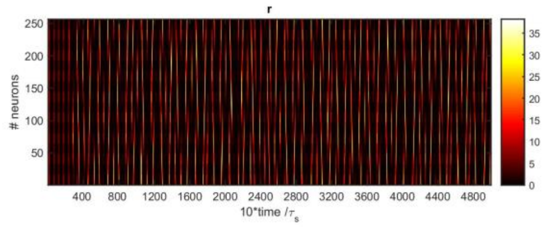

(3) Beta = 0.25: Mixed

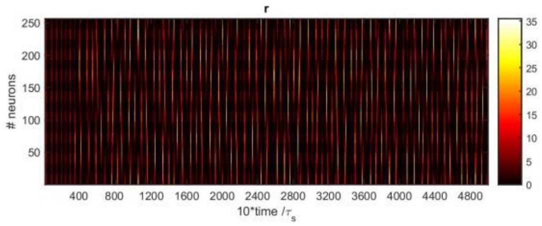

(4) Beta = 0.35: Mixed, spikes moving slower

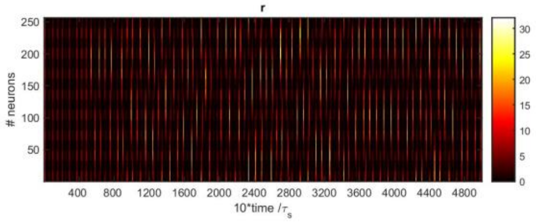

(5) Beta = 0.45: Mixed, spikes moving even slower, providing sense of continuity

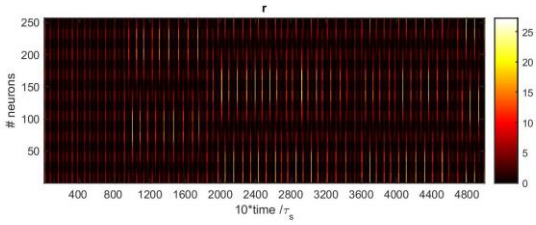

(6) Beta = 0.55: Spikes, occasionally moving

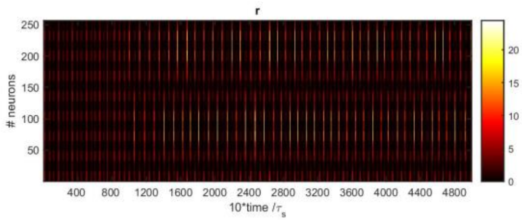

(7) Beta = 0.65: Spikes, staying steady

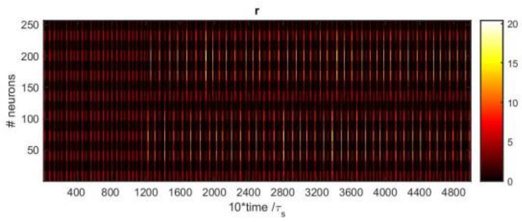

(8) Beta = 0.75: Spikes, staying steady

Figure 4

The above set of images clearly shows the impact of increasing beta value, or the degree of synaptic depression. **First, larger beta slows down the state evolution.** State evolution usually proceeds in an order of 'homogeneous spike', 'spike', and then to 'mixed' or 'rotating bump'. It is possible to see that the period of initial homogeneous spike state is getting longer and longer as beta value increases. **Second, larger beta makes the rotating bump faster. Third, larger beta restricts the spatial movement of spikes.** Intuitively, these two effects can be metaphorically understood by considering the neural ring as a rope with its tension related with beta and height of its differential component related with the firing rate. Since stronger tension makes the pulse on the rope move faster by making the up and down components of the pulse shape more elastic. This explains the second effect, and the third effect can be partially explained by that high beta value strongly restricts the neurons nearby the ones that recently formed spike, making the only possible neuron position for the next spike be the exactly opposite side of the previous spike.

The effect of varying global inhibition can be studied from table 1 and another observation that **larger k makes the rotating bump slower**. While the table 1 suggests that k and beta might affect the system in an equivalent manner, the observation emphasizes its oppositeness from beta. Again, metaphorically, setting a larger k is comparable to putting the ring into a more viscous liquid. In that sense, the global inhibition (k) and short-term synaptic depression (beta) have distinct role in supporting the neural network dynamics, especially in that one influences globally, while the other influences locally

4. References

[1] R. Sokoliuk and R. VanRullen, "The flickering wheel illusion: when α rhythms make a static wheel flicker," *J. Neurosci. Off. J. Soc. Neurosci.*, vol. 33, no. 33, pp. 13498–13504, Aug. 2013.
[2] N. A. Busch and R. VanRullen, "Spontaneous EEG oscillations reveal periodic sampling of visual attention," *Proc. Natl. Acad. Sci.*, vol. 107, no. 37, pp. 16048–16053, 2010.
[3] N. A. Busch, J. Dubois, and R. VanRullen, "The phase of ongoing EEG oscillations predicts visual perception," *J. Neurosci.*, vol. 29, no. 24, pp. 7869–7876, 2009.
[4] C. A. Fung, K. M. Wong, and S. Wu, "Dynamics of neural networks with continuous attractors," *EPL Europhys. Lett.*, vol. 84, no. 1, p. 18002, 2008.
[5] H. Wang, K. Lam, C. C. A. Fung, K. Y. M. Wong, and S. Wu, "A Rich Spectrum of Neural Field Dynamics in the Presence of Short-Term Synaptic Depression," *ArXiv150203662 Cond-Mat Q-Bio*, Feb. 2015.